24 July 2002

ELSEVIER

Chemical Physics Letters 361 (2002) 42–48

CHEMICAL PHYSICS LETTERS

www.elsevier.com/locate/cplett

Energy transfer between two kinds of J-aggregates studied by near-field absorption-fluorescence spectroscopy

Naoki Fukutake, Shigehiro Takasaka, Takayoshi Kobayashi *

Department of Physics, Faculty of Science, University of Tokyo, 7-3-1 Hongo, Bunkyo, Tokyo 113-0033, Japan

Received 28 June 2001; in final form 7 May 2002

Abstract

A layer sample of J-aggregates of the dye pseudoisocyanine bromide in an ethylene glycol/water glass layer was studied by scanning near-field optical microscopy (SNOM) developed in our group. The absorption and fluorescence spectra of the sample were measured at 50×50 scanned sample points at 8 K. The fluorescence dynamics was measured by the optical Kerr-gate method, which verified the excitation-energy transfer to optically forbidden states. © 2002 Elsevier Science B.V. All rights reserved.

1. Introduction

J-aggregates are of interest from both application and fundamental viewpoints. The J-aggregates of cyanine dyes are widely used in silver halide photography as a spectral sensitizer [1,2]. They are regarded in solid-state physics and chemistry as an important model for one-dimensional molecular exciton [3]. J-aggregates exhibit a sharp characteristic absorption peak, the so-called J-band, which is red-shifted to the monomer absorption band due to the delocalization of excitation over an aggregate by intermolecular interaction between (most effectively nearest-neighboring) two transition dipole moments. The J-aggregates also offer an excellent model to study photophysical processes such as excitation energy transfer important in the light collection mechanism of photosynthetic antenna systems [4–7]. Scanning near-field optical microscopy (SNOM) provides a useful tool to directly probe the optical properties of J-aggregates with a spatial resolution. We have recently developed a novel SNOM system that can measure absorption and fluorescence spectra at 50×50 scanned sample points at low temperature and the details of the system is described previously [8].

Pseudoisocyanine bromide (PIC-Br) in ethylene glycol/water glass (EGWG) is known to exhibit two sharp transition bands at 2.152 and 2.174 eV when it is rapidly cooled [9–11]. Several ideas about the origin of these bands have been suggested since the discovery of J-band splitting by Cooper [9]. Some reports claimed that these bands were due to the two aggregates in different structures [12,13] or that the J-band splitting was ascribable to the excitonic interactions between at

* Corresponding author. Fax: +81-3-5841-4165.
E-mail address: kobayashi@phys.s.u-tokyo.ac.jp (T. Kobayashi).

0009-2614/02/$ - see front matter
PII: S0009-2614(02)00882-5

least two linear J-aggregates [14]. The energy transfer between these aggregates composed of the same cyanine dye molecules was suggested to explain the close resemblance between the absorption spectrum and the fluorescence-excitation spectrum [15]. The energy transfer process between the J-aggregates was investigated in two-dimensional systems of J-aggregates such as Langmuir–Blodgett films [16,17] and three-dimensional systems doped in a polymer matrix [18]. In such systems the spectral overlap of donor fluorescence and acceptor absorption is essential for efficient transfer. In the present Letter the energy-transfer mechanism between the donor and accepter aggregates is discussed in the case of the absence of the overlap of these spectra.

2. Experimental

Pseudoisocyanine bromide (PIC-Br: Japanese Research Institute for Photosensitizing Dyes, 1-ethyl-2-[(1-ethyl-2(1H)-quinolylidene)methyl]quinolinium bromide), ethylene glycol (Kanto Chemical), and polyvinylalcohol (PVA: Kanto Chemical) were used without further purification. PIC-Br (4×10^{-3} mol) and PVA (5 mg) was dissolved in 2 ml water/ethylene glycol (volume mixture 1:1) at 90 °C. To make a film sample, hot solution was spin-coated on a fused-quartz microscope-coverglass at 6000 rpm. Just after spin coating, the sample was rapidly cooled down to 8 K in a few minutes.

The laser system for the optical Kerr-gate method was composed of a mode-locked Ti:sapphire laser (Clark-MXR, NJA-4) pumped with an argon-ion laser and a regeneretive amplifier (Clark-MXR, CPA-1000) pumped by a Nd:YAG laser (ORC-1000). The output from the Ti:sapphire regenerative amplifier (818 nm, 100 fs, 350 μJ, and 1 kHz) was divided into two for excitation and gate pulses. The second harmonic (409 nm, 2.8 GW/cm^2, and 5.8×10^{14} photons/cm^2) generated by a 3-mm-thick LBO crystal was used as the excitation pulse. The gate-pulse intensity and peak power density were 200 μJ and 70 GW/cm^2, respectively. Carbon disulfide in a 1-mm-thick cell was used as the Kerr-medium. The time-resolved fluorescence was spectrally dispersed by a polychromator (SPEX, 320) and detected by a CCD camera with an image intensifier (Hamamatsu Photonics, C4880). The gate time for the image intensifier was 5 ns. The time resolution of this system was determined to be 1.1 ps by measuring gate-time dependence of the detected intensity of the excitation pulse scattering from a glass plate placed at the sample position instead of the sample.

3. Results and discussion

3.1. Energy transfer between two kinds of J-aggregates

The absorption and fluorescence spectra of the present sample of J-aggregates in the EGWG thin film show two intense narrow bands with maxima at 2.152 (red-band) and 2.174 eV (blue-band) at low temperature. The photon energies of both absorption and fluorescence bands agree within 5 meV with those reported [10,11] for the bulk sample. These bands show essentially no Stokes shifts [10,11], smaller than 1 meV if any; they may be caused by residual reabsorption effect. Because the relative intensities of these bands in absorption and fluorescence depend on the cooling rate of the sample, the two bands can be ascribed to different aggregate structures. Hereafter, the two aggregates are referred to as blue- and red-aggregates, respectively. The excitation fluorescence spectra probed at these bands measured at 77 K, shown in Fig. 1, have common spectral features except for a relative shift of about 150 cm^{-1} [15]. However, the excitation spectrum probed at red-band contains both blue- and red-band absorption spectra. This fact suggests the excitation energy transfer from the blue-aggregates to the red. During the relaxation down to the lowest electronic excited state (J-band) after excitation, energy transfer from the blue- to red-aggregates and the reverse can take place. However, intraband relaxation rates in the respective aggregates are much higher than the energy transfer rate. Therefore, the energy transfer from the blue- to red-aggregates takes place dominantly after the relaxation down to the bottom of the J-band.

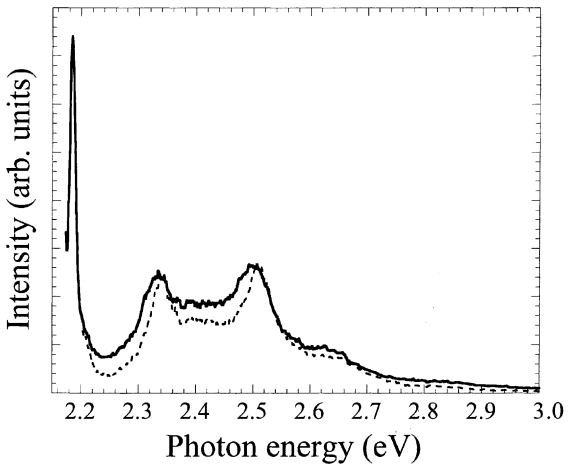

Fig. 1. Excitation fluorescence spectra of structurally different aggregates of PIC-Br in ethylene glycol/water glass probed at red-band (solid curve) and blue-band (dashed curve) measured at 77 K.

The dynamics of excitation-energy transfer from the blue- to the red-aggregates were studied by time-resolved fluorescence spectroscopy at 4 K using an optical Kerr-gate. The decay curve of the red-band, shown in Fig. 2, indicates that the fluorescence of this component has a delayed growth with respect to that of the blue-band. The rise time of the blue-band emission is consistent with the time resolution (1.1 ps) of the detection system, whereas that of the red-band is significantly longer because of the excitation energy transfer from the blue- to red-aggregates. The details of the result will be published elsewhere.

The absorption and fluorescence spectra at the 50×50 pixels, which scanned the same sample positions, were measured with the SNOM at 8 K after five selected points were illuminated for 1 min by the second harmonic (532 nm) of the Nd:YAG laser. The transmitted laser intensity deposited on the sample points was about 100 kW/cm^2. Near-field fluorescence spectra and images were obtained using the excitation of 532 nm (2.33 eV), as shown in Fig. 3. The dark regions of the fluorescence image in Fig. 3b indicate that the fluorescence is reduced by the laser illumination induced by defect formation. Conceivable defects are caused by covalently bound species, from dimers

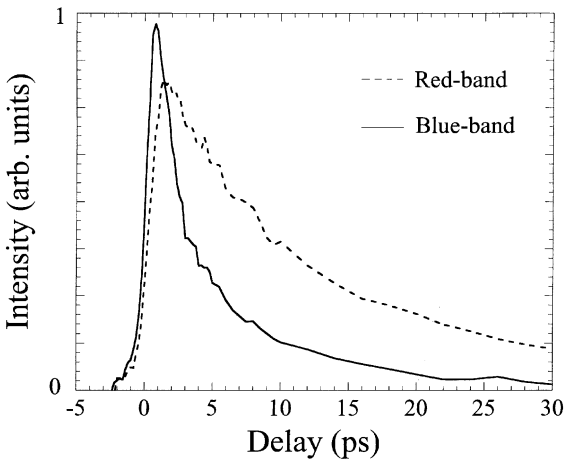

Fig. 2. Gate-delay time dependence of the fluorescence intensities of the red-band probed at 2.152 ± 0.002 eV (dotted curve) and that of the blue-band at 2.174 ± 0.002 eV (solid curve).

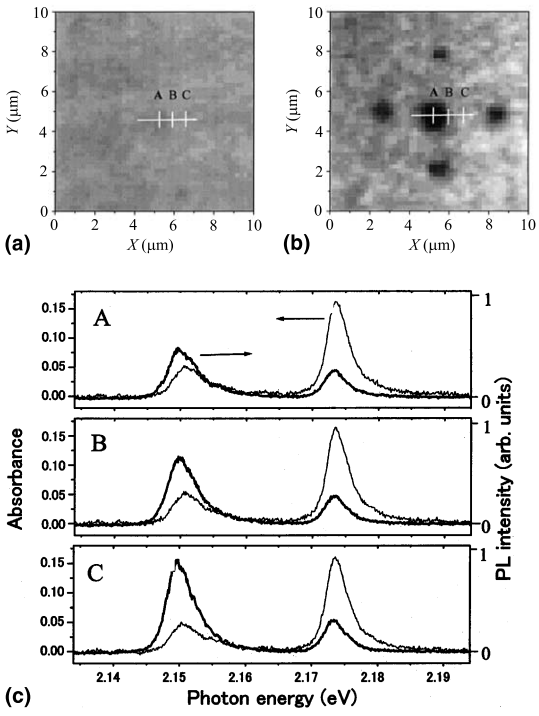

Fig. 3. Near-field (a) absorption and (b) fluorescence images (10×10 μm^2) constructed from integrating the intensity around the peak at 2.152 eV (red-band) and (c) near-field absorption (thin curve) and fluorescence (thick curve) spectra at the same points A, B, and C in the images.

to oligomers with extended conjugation length. However, the absorption images are hardly affected at any of these five regions. No detectable effect of pre-illumination was observed in the absorption and fluorescence images generated from the integrated intensity around the blue-band peak (not shown).

3.2. Estimation of energy-transfer rate by near-field spectroscopy

Although the absorption spectra at all scanned points are similar, the peak intensity ratios of the two fluorescence bands are quite different. Fractions of blue- and red-aggregates form defects in Fig. 3b, indicating reduction of the fluorescence quantum yield of these bands. The quantum efficiency for the red-aggregates is reduced more drastically than that for the blue-aggregates, probably for the following reason. After a coherent aggregate (mesoaggregate) [19,20] is excited, the transfer of excitation energy to neighboring mesoaggregates belonging to the same family of either blue- or red-aggregates can compete with exciton superradiance and radiationless relaxation. Since the fluorescence quantum yield of the blue-aggregates is reduced by energy transfer to the red-aggregates, the creation of additional defects does not substantially affect the quantum yield of the blue-aggregates. On the other hand, that of the red-aggregates is decreased more significantly by the existence of the defects.

The energy transfer rate $T_{B\to R}$ from the blue- to red-aggregates affects the fluorescence spectrum. The quantum yields of the blue- and red-aggregates to the number of total absorbed photons are given by

$$\Phi_{\text{blue}} = \frac{f_{\text{blue}} \cdot B_r}{B_r + B_{nr} + B_d + T_{B\to R}}, \tag{1}$$

$$\Phi_{\text{red}} = \frac{R_r}{R_r + R_{nr} + R_d} \times \left(f_{\text{red}} + \frac{f_{\text{blue}} \cdot T_{B\to R}}{B_r + B_{nr} + B_d + T_{B\to R}} \right). \tag{2}$$

Here, B_r, B_{nr}, and B_d are the radiative decay rates, non-radiative decay rate, and the trapping rate to the defects for the blue-aggregates with the fraction of f_{blue}, respectively. R_r, R_{nr}, and R_d are the corresponding rates for the red-aggregates with the fraction of f_{red}.

The absorption intensities of blue- and red-bands are nearly equal regardless of the presence of laser radiation. However, the fluorescence intensity of the red-band in the dark region in Fig. 3b decreases by about 50% in the bright region. The corresponding decrease for the blue-band is about 15%. These estimates indicate that Φ_{blue} is insensitive to the increase in B_d but Φ_{red} is sensitive to that in R_d. R_d can be estimated from Eq. (2) to be nearly equal to $R_r + R_{nr}$. Assuming that B_d is in the same order as R_d, $T_{B\to R}$ is estimated from Eq. (1) to be several times larger than $B_r + B_{nr}$. The decay times are assumed from time-resolved fluorescence spectroscopy (Fig. 2) to be $1/(R_r + R_{nr}) = 1/(B_r + B_{nr}) = 15$ ps; therefore, the transfer time is estimated as $1/T_{B\to R} = 5 \pm 2$ ps. Thus the drastic difference in the relative intensities of the two bands between absorption and fluorescence spectra at the same points in Figs. 3a,b indicates that the energy transfer from the blue- to the red-aggregates takes place very efficiently. The energy transfer rate $T_{B\to R}$ estimated above is discussed in the following section.

3.3. Calculation of energy-transfer rate

Because the overlap between the blue-band of the fluorescence spectrum and the red-band of the absorption spectrum (Fig. 3) is negligible, the energy-transfer rate from blue-band to red-band (optically allowed state) due to Förster mechanism [21,22] is estimated to be much smaller than 10^7 s^{-1}. However, the energy transfer rate from blue-band to the higher one-exciton state of red-aggregates (optically forbidden state), shown in Fig. 4c, can have finite values if the distance between the two kinds of aggregates is smaller than the exciton delocalization size of J-aggregates. To describe the energy-transfer process, the transition dipole of the aggregate cannot be simply represented by using a transition dipole in the point-dipole approximation by summing all the individual transition dipoles in the aggregate. The individual molecules in the blue- and red-aggregates have nonvanishing transition dipoles.

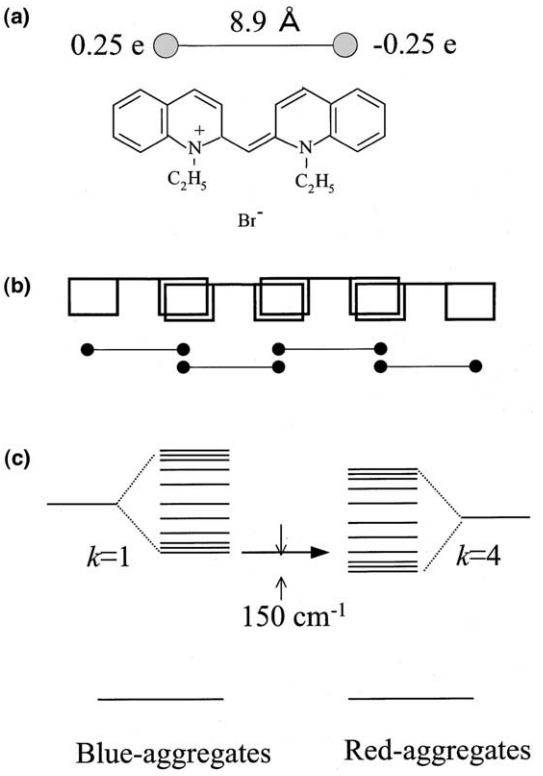

Fig. 4. (a) Structure of a PIC-Br molecule and a model of extended transition dipole moment, (b) geometrical configuration of J-aggregate accepted generally and arrangement of extended dipole moment assumed for the calculation of transition moment, and (c) scheme of energy levels of the red- and blue-aggregates where the ground states are assumed to have the same energy.

Therefore, even when their sum vanishes completely at an exciton state forming an optically forbidden state, the energy transfer to the optically forbidden state of the red-aggregates can take place due to interactions between the individual transition dipoles in the blue- and red-aggregates [7,23].

For calculation of the energy-transfer rate, the transition moments of J-aggregates are approximated by multipole moments as shown in Fig. 4b, and Kuhn's model is used for the transition dipole moment of a molecule. It is given by $M = Ql$ with charge, Q, and the π-electron delocalization length, l, as shown in Fig. 4a, where $Q = 0.25e$ (e: electron charge) and $l = 8.9$ Å are assumed [3,24]. This approximation is simple but still useful at a short distance between the two types of aggregates. Under the further assumption that the vibrational relaxation is completely terminated before the energy transfer, the vibrational population distribution of the initial state follows the Boltzmann distribution. The energy-transfer rate $T_{B\to R}$ is then given by

$$T_{B\to R} = \frac{2\pi}{\hbar} U^2 \int D(E)A(E)\,dE, \tag{3}$$

$$D(E) = \frac{1}{Z'_d} \sum_{v'_d} \sum_{v_d} \exp\left(-\frac{E_d^{v'}}{k_B T}\right) |\langle v'_d | v_d \rangle|^2 \times \delta(E - \epsilon_d - E_d^{v'} - E_d^{v}), \tag{4}$$

$$A(E) = \frac{1}{Z_a} \sum_{v'_a} \sum_{v_a} \exp\left(-\frac{E_a^{v}}{k_B T}\right) |\langle v'_a | v_a \rangle|^2 \times \delta(E - \epsilon_a - E_a^{v'} - E_a^{v}). \tag{5}$$

Here, v' and v denote the vibrational levels on the excited and ground states, and subscripts d and a mean the donor (blue-) and acceptor (red-) aggregates, respectively; ϵ is the 0–0 transition energy, Z' and Z are the partition functions of the excited and ground state, respectively, as given by

$$Z'_d = \sum_{v'_d} \exp\left(-\frac{E_d^{v'}}{k_B T}\right), \quad Z_a = \sum_{v_a} \exp\left(-\frac{E_a^{v}}{k_B T}\right). \tag{6}$$

$D(E)$ in Eq. (4) is given by the normalized fluorescence spectrum of the donor aggregates, and $A(E)$ in Eq. (5) represents the density of the vibrational levels coupled to the exciton state in the acceptor aggregates. U is the Coulomb interaction between the transition moments of the donor and accepter aggregates. For the calculation of U, a dielectric constant of 2.5 is used. In this model the transition moment of the J-aggregate is a linear multipole moment as shown in Fig. 4b. The transition moment can be found from the eigenvector of the kth exciton state through the diagonalization of the Hamiltonian of one-exciton state H

$$H = \epsilon \sum_{i=1}^{N} |n\rangle\langle n| + J \sum_{i=1}^{N-1} (|n\rangle\langle n+1| + |n+1\rangle\langle n|). \tag{7}$$

In brief, the transition dipole moments of each molecule in the J-aggregate are proportional to the elements of the eigenvectors. Consequently, the charges of the dipole moments presented as filled circles in Fig. 4b can be found. Suppose that the neighboring point charges overlap with each other. The eigenvalues E_k of Hamiltonian H and the corresponding eigenvectors $|k\rangle$ are given by

$$E_k = \epsilon + 2J\cos\left(\frac{\pi k}{N+1}\right), \quad (k = 1, 2, \ldots, N), \tag{8}$$

$$|k\rangle = \sqrt{\frac{2}{N+1}}\sum_{n=1}^{N}\sin\left(\frac{n\pi}{N+1}k\right)|n\rangle, \quad (k = 1, 2, \ldots, N). \tag{9}$$

Here, $|n\rangle$ denotes the configuration in which only the nth molecule is in the excited state while the other molecules are in the ground state. ϵ is the transition energy of the molecule, J is the transfer interaction matrix element between two neighboring molecules, N is the number of the molecules in the aggregate. In this calculation $N = 20$ and $J = -600$ cm^{-1} were used.

The one-exciton state of $k = 1$ occupies most of the oscillator strength and the other states have much smaller oscillator strength. The eigenvalues E_k are different by 150 cm^{-1} between the blue- and red-aggregates as shown in Fig. 4c. Because of the energy conservation, the energy transfer between the lowest exciton states ($k = 1$) of the blue- and red-aggregates is impossible. For $N = 20$, $J = -600$ cm^{-1}, $D(E)$ has the largest overlap with the density of vibrational levels coupled to the fourth lowest exciton state ($k = 4$) in the acceptor aggregates. Because of the very narrow band widths ($\leqslant 50$ cm^{-1}) of the absorption and fluorescence spectra, the integration $\int D(E)A(E)\,\mathrm{d}E$ in Eq. (3) can be very large ($\geqslant 10^{-3}$ cm), so the energy transfer rate $T_{B\to R}$ can be larger than the exciton superradiance rate. Fig. 5 shows the dependence of the energy-transfer rate on the distance between the blue- and red-aggregates in the transfers from the lowest one-exciton state of the blue-aggregates to the four states of the red-aggregates. In each case, it is assumed that the energy levels of the initial state of the blue-aggregate and the final state of the red-aggregate are within the band width caused by the vibrations being coupled to each exciton mode. In this model, the blue- and red-aggregates are parallel as shown in Fig. 5e. In this calculation, the value of the integration, $\int D(E)A(E)\,\mathrm{d}E$, is assumed to be 5×10^{-3} cm in each case shown in Fig. 5. The higher exciton states are optically forbidden, but the interaction energy between the transition moments of the $k = 1$ state in the blue-aggregate and a higher state in the red-aggregate has a finite value if the distance between these aggregates is shorter than 30 Å (see Fig. 5d). The exciton state in which the density function of the vibrational levels of the red-aggregates has the largest overlap with the fluorescence spectrum of the blue-aggregates

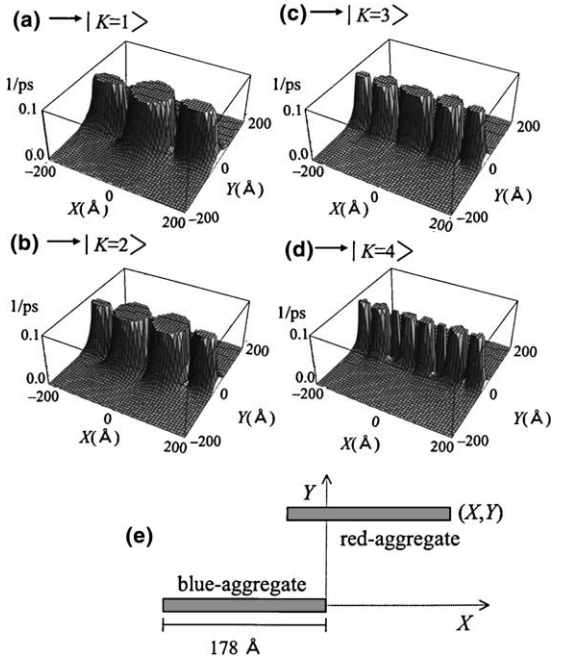

Fig. 5. Dependence of the energy-transfer rate on the distance between the blue- and red-aggregates; transfer from the $k = 1$ state of the blue-aggregates to (a) the $k = 1$ state, (b) the $k = 2$ state, (c) the $k = 3$ state, and (d) the $k = 4$ state of the red-aggregates. The integration $\int D(E)A(E)\,\mathrm{d}E$ of Eq. (3) is assumed to be 5×10^{-3} cm in all cases. (e) Structural model of the neighboring aggregates in the parallel configuration of blue- and red-mesoaggregates.

depends on the parameters N and J, but the energy can be transferred with a high rate to any of the exciton states. The results shown in Fig. 5 reveal the excitation energy transfer from the lowest one-exciton state of the blue-aggregates to an upper exciton state (optically forbidden state) of the red-aggregates. The distance between the center of the aggregates, or an averaged distance, can be estimated from the concentration of the dye to be about 25 Å. Then the rate of energy transfer from the $k = 1$ state of the blue-aggregates to the $k = 4$ state of the red-aggregates is calculated to be $1/T_{B\to R} \approx 8$ ps. This calculation includes explicit consideration of the transition moments of two randomly orientated aggregates. The present estimate, 8 ps, is in reasonable agreement with the estimated value of 5 ± 2 ps in Section 3.2, if we take account of the simplicity of the model.

4. Conclusion

J-aggregates of pseudoisocyanine bromide in EGWG, studied by the SNOM and optical Kerr-gate method, have revealed that the energy transfer between two kinds of J-aggregates takes place rapidly. The energy-transfer rate from the lowest exciton state of the blue-aggregates to the higher exciton state (optically forbidden state) of the red-aggregates is estimated to be 5 ± 2 ps. The estimated value of the energy-transfer rate is close to the calculation, 8 ps.

Acknowledgements

The authors are grateful to Dr. E. Tokunaga for his careful reading of the manuscript and Kawaguchi Optical Industries for the preparation of fiber tips. The work is partly supported by Research for the Future of Japan Society for the Promotion of Science (JSPS-RFTF-97P-00101).

References

[1] T. Tani, T. Suzumoto, K. Kemnitz, K. Yoshihara, J. Phys. Chem. 96 (1992) 2778.
[2] A.A. Muenter, D.V. Brumbaugh, J. Apolito, L.A. Horn, F.C. Spano, S. Mukamel, J. Phys. Chem. 96 (1992) 2783.
[3] T. Kobayashi, J-Aggregates, World Scientific, Singapore, 1996.
[4] J.T.M. Kennis, A.M. Streltsov, H. Permentier, T.J. Aartsma, J. Amesz, J. Phys. Chem. B 101 (1997) 8369.
[5] R. Monshouwer, I. Ortiz de Zarate, F. van Mourik, R. van Grondelle, Chem. Phys. Lett. 246 (1995) 341.
[6] V. Nagarajan, W.W. Parson, Biochemistry 36 (1997) 2300.
[7] K. Mukai, S. Abe, H. Sumi, J. Lumin. 87–89 (2000) 818.
[8] N. Fukutake, S. Takasaka, T. Kobayashi, J. Appl. Phys. 91 (2002) 849.
[9] W. Cooper, Chem. Phys. Lett. 7 (1970) 73.
[10] S. De Bore, K.J. Vink, D.A. Wiersma, Chem. Phys. Lett. 137 (1887) 99.
[11] H. Fidder, J. Knoester, D.A. Wiersma, Chem. Phys. Lett. 171 (1990) 529.
[12] D.L. Akins, J.W. Mackline, J. Phys. Chem. 93 (1989) 5999.
[13] R. Hirschmann, W. Köhler, J. Friedrich, E. Daltrozzo, Chem. Phys. Lett. 151 (1988) 60.
[14] H. Ito, M. Agatsuma, Y.J. I'Haya, Bull. Chem. Soc. Jpn. 64 (1991) 3700.
[15] S. De Boer, D.A. Wiersma, Chem. Phys. Lett. 165 (1990) 45.
[16] T.L. Penner, Thin Solid Films 160 (1988) 241.
[17] Y. Yonezawa, H. Kurokawa, T. Sato, J. Lumin. 54 (1993) 285.
[18] M.I. Sluch, A.G. Vitukhnovsky, Y. Yonezawa, T. Sato, T. Kunisawa, Opt. Mater. 6 (1996) 261.
[19] T. Kobayashi, K. Misawa, J. Lumin. 72–74 (1997) 38.
[20] T. Kobayashi, Supramolec. Sci. 5 (1998) 343.
[21] T. Förster, Ann. Phys. (Leipzig) 2 (1948) 55.
[22] D.L. Dexter, J. Chem. Phys. 21 (1953) 836.
[23] H. Sumi, J. Phys. Chem. B 103 (1999) 252.
[24] V. Czikkely, H.D. Försterling, H. Kuhn, Chem. Phys. Lett. 6 (1970) 207.